Stress and morphology of a nonpolar *a*-plane GaN layer on *r*-plane sapphire substrate*

Xu Sheng-Rui(许晟瑞)[a)†], Hao Yue(郝 跃)[a)], Zhang Jin-Cheng(张进成)[a)], Xue Xiao-Yong(薛晓咏)[a)], Li Pei-Xian(李培咸)[b)], Li Jian-Ting(李建婷)[c)], Lin Zhi-Yu(林志宇)[a)], Liu Zi-Yang(刘子扬)[a)], Ma Jun-Cai(马俊彩)[a)], He Qiang(贺 强)[b)], and Lü Ling(吕 玲)[a)]

[a)] *Key Laboratory of Wide Band-Gap Semiconductor Technology, School of Microelectronics, Xidian University, Xi'an* 710071, *China*

[b)] *School of Technical Physics, Xidian University, Xi'an* 710071, *China*

[c)] *Zoomview Oprtoelectronic, Co., LTD, Xi'an* 710065, *China*

(Received 24 May 2011; revised manuscript received 5 July 2011)

The anisotropic strain of a nonpolar $(11\bar{2}0)$ *a*-plane GaN epilayer on an *r*-plane $(1\bar{1}02)$ sapphire substrate, grown by low-pressure metal-organic vapour deposition is investigated by Raman spectroscopy. The room-temperature Raman scattering spectra of nonpolar *a*-plane GaN are measured in surface and edge backscattering geometries. The lattice is contracted in both the *c*- and the *m*-axis directions, and the stress in the *m*-axis direction is larger than that in the *c*-axis direction. On the surface of this sample, a number of cracks appear only along the *m*-axis, which is confirmed by the scanning electron micrograph. Atomic force microscopy images reveal a significant decrease in the root-mean-square roughness and the density of submicron pits after the stress relief.

Keywords: crystal morphology, nonpolar GaN, Raman, metal-organic chemical vapour deposition

PACS: 78.55.Cr, 81.15.Kk **DOI:** 10.1088/1674-1056/20/10/107802

1. Introduction

Gallium nitride and its alloys with indium and aluminum nitride are very attractive materials due to their wide range of applications in opto-electronic and electronic devices. The majority of conventional GaN devices are grown with respect to the *c*-plane grown on *c*-plane sapphire and SiC. The polarization field in a multiple quantum well structure along the polar *c* axis causes significant band bending and thus gives rise to spatial separation between electrons and holes. This situation leads to reduced optical emission efficiency of light-emitting diodes (LEDs), as well as an undesirable redshift in the emission spectrum from the quantum well.[1] This problem can be avoided by growing GaN in nonpolar orientations, such as *a* plane and *m* plane, in which the polar *c* axis is at 90° with respect to the growth direction. Therefore, recently, there has been considerable interest in the growth of nonpolar gallium nitride based on epitaxial films, heterostructures and devices.[2−7] However, it is extremely difficult to grow nonpolar GaN on *r*-sapphire due to a number of challenges. Previous reports have shown that a dislocation density of $\sim 10^{10}$ cm^{-2} and a basal plane stacking fault (BSF) of $\sim 10^{5}$ cm^{-1} are found in nonpolar *a*-plane GaN under different growth conditions, which was believed to limit the room temperature internal quantum efficiency of nonpolar InGaN/GaN structures.[5−7] Furthermore, many structural properties resulting from the heteroepitaxial growth in the *a*- and *m*-directions are not well understood. For example, in-plane stress, which affects various important device parameters, can be very complex. The stress is expected to be anisotropic due to the anisotropies in the thermal expansion coefficients of the layer and the substrate, as well as the anisotropies in the elastic and plastic stress relief mechanisms.[8] To properly determine residual stress in synthesized GaN thin films with high spatial resolution, micro-Raman spectroscopy has been extensively applied to *c*-plane GaN due to its simplicity and nondestructive nature.[9−13] All of these stud-

*Project supported by the National Key Science and Technology Special Project, China (Grant No. 2008ZX01002-002), the Major Program and State Key Program of National Natural Science Foundation of China (Grant Nos. 60890191 and 60736033), and the Fundamental Research Funds for the Central Universities, China (Grant No. JY10000904009).

†Corresponding author. E-mail: shengruixidian@126.com

© 2011 Chinese Physical Society and IOP Publishing Ltd

ies indicate that Raman scattering is a powerful tool for investigating the epitaxial growth characteristics of GaN-based thin film heterostructures. However, until now, there have been few studies of the strain state of nonpolar a-plane GaN along the c and m planes by Raman scattering spectroscopy. Particularly, knowledge of the influence of stress on morphology is very scarce. Here, we report an investigation of the nonpolar a-plane GaN phonon anisotropy by direction-dependent Raman spectroscopy. The study will be helpful for a deep understanding of the relationship between the morphology and strain of nonpolar a-plane GaN.

2. Experimental procedure

Hexagonal wurtzite GaN is a tetrahedrally coordinated semiconductor compound and belongs to the space group C_{6v}^4. All its atoms occupy sites of symmetry C_{3v}.[13,14] The a-plane GaN films were grown on r-plane $(1\bar{1}02)$ sapphire substrates using a cold-wall shower head metal-organic chemical vapour deposition (MOCVD) system. After chemical cleaning, r-plane sapphire substrates were loaded into the chamber. H_2 was used as the carrier gas and triethylgallium, trimethylaluminium and ammonia (NH_3) were used as source compounds. A low temperature AlN (LT-AlN) nucleation layer of 25 nm and a high-temperature AlN (HT-AlN) layer of 100 nm were grown at 620 °C and 1050 °C, respectively. After buffer layer growth, a 7.5-μm-thick a-plane GaN epitaxial layer was grown at 1020 °C. For the Raman testing, by using a spectrograph with a single grating monochromator, a spectral resolution of 0.5 cm^{-1} was achieved. The wavelength of the excitation laser was 514 nm and the laser power was about 3.5 mW. The surface morphology of the sample was recorded by using a scanning electron microscope (SEM) and atomic force microscopy (AFM) operated in tapping mode.

3. Results and discussion

Raman scattering is widely used to investigate hexagonal wurtzite GaN films grown on sapphire substrates, owing to it being nondestructive and contactless. According to the polarization selection rules, the scattering configurations, E_2 (high), A_1 (TO), and A_1 (LO) phonon modes, can be observed.[15] In the Raman scattering study of c-plane GaN, the scattering geometry (the x and the y axes) can be arbitrarily chosen in the plane because the a axis and the m axis are isotropic. However, there are in-plane anisotropies in the surface, the strain and the crystalline quality of a-plane GaN, so the coordinate axes should be parallel to the corresponding crystal orientations, here $x||(11\bar{2}0)$, $y||(1\bar{1}00)$, and $z||(0001)$.

Figure 1 displays Raman spectra acquired in the backscattering geometry from the sample surface for the configurations $x(yy)$–x, $x(yz)$–x and $x(zz)$–x, showing that there are two main peaks located at 534 cm^{-1} and 570.3 cm^{-1} in the $x(yy)$–x configuration, two peaks located at 561 cm^{-1} and 570.6 cm^{-1} in the $x(yz)$–x configuration and one peak located at 534 cm^{-1} in the $x(yy)$–x configuration. The peaks near 532, 559, and 570 cm^{-1} are A_1(TO), E_1 (TO), and E_2 (high), respectively. Generally, the E_2 (high) phonon mode provides useful information about crystalline quality and stress in the heteroepitaxial GaN structure. Therefore, we mainly focus on the E_2 (high) phonon mode under different configurations.

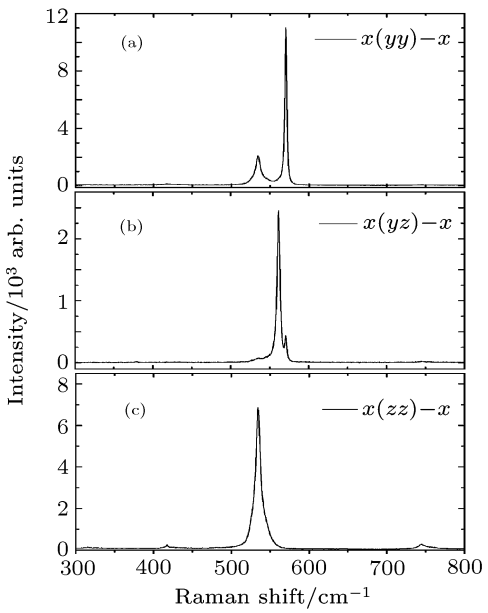


Fig. 1. Raman scattering spectra of nonpolar a-plane GaN from the surface geometry in three backscattering configurations: (a) $x(yy)$–x, (b) $x(yz)$–x, and (c) $x(zz)$–x.

In order to study the anisotropic strain, the Raman scattering spectra are measured from the edge backscattering geometries. Figure 2 shows the Raman scattering spectra of nonpolar a-plane GaN in $y(xx)$–y, $y(xz)$–y, and $y(zz)$–y configurations. Figure 3 shows the Raman scattering spectra in $z(xx)$–z, $z(xy)$–z, and $z(yy)$–z configurations. Compared with in the $x(\ )$–x mode, a significant difference in the Raman spectrum is that the A_1 (LO) phonon mode at

740 cm^{-1} appears in each of the $z(xx)$–z mode and the $z(yy)$–z mode. Generally, the A_1 (LO) phonon mode corresponds to the normal mode along the c axis, which is consistent with our Raman geometry configurations and in accordance with the selection rules. It should be noted that the frequency values of E_2 (high) modes measured from the modes $x()$–x, $y()$–y and $z()$–z have a great differences among them as shown in Fig. 4. This reveals that the strain distribution in the nonpolar a-plane GaN is anisotropic. Furthermore, once the direction of the incident light is fixed, the variation of the E_2 (high) mode with the polarization direction is not significant. So the anisotropic strain should be calculated according to the direction of incident light.

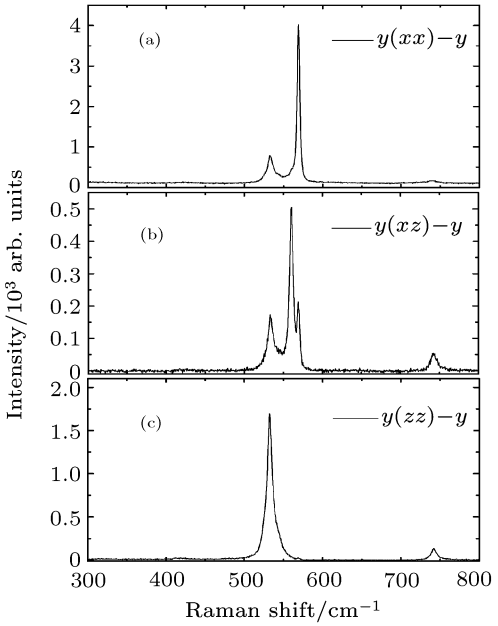


Fig. 2. Raman scattering spectra of nonpolar a-plane GaN from the surface geometry in three backscattering configurations: (a) $y(xx)$–y, (b) $y(xz)$–y, and (c) $y(zz)$–y.

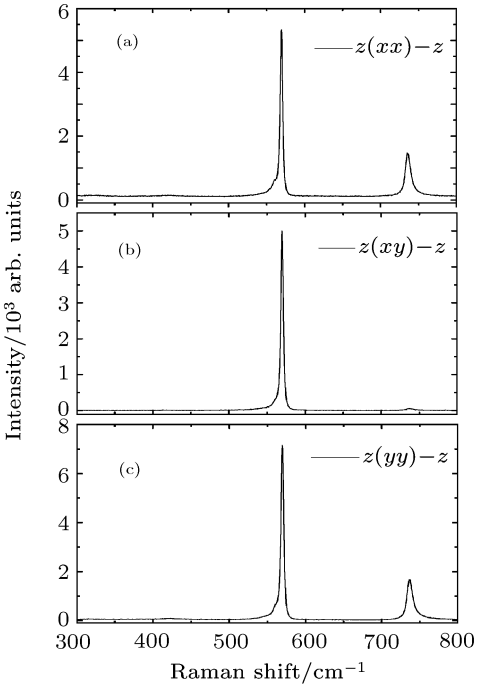


Fig. 3. Raman scattering spectra of nonpolar a-plane GaN from the surface geometry in three backscattering configurations: (a) $z(xx)$–z, (b) $z(xy)$–z, and (c) $z(yy)$–z.

It is well known that the frequency of the E_2 (high) mode is sensitive to strain, as expected from the atomic displacement scheme of N atoms, in which the displacement is perpendicular to the c axis.[16] The E_2 (high) mode appears 7 times among the 9 backscattering configurations according to the Raman results above. The specific frequencies of the E_2 (high) modes are shown in Fig. 4. The frequency values of the E_2 (high) modes measured from the surface geometry and edge geometry differ from each other largely. A larger in-plane compressive strain can be found in the surface than in the edge as compared with the frequency value of the E_2 (high) mode of strain-free GaN. The average E_2 (high) phonon modes of a-plane GaN under the configurations of $x(\,)$–x and $z(\,)$–z are located at 570.47 cm^{-1} and 569.5 cm^{-1}, respectively. Using a reference frequency of 568 cm^{-1} with a value of 2.7 cm^{-1}/GPa as a linear proportionality factor between the shift in the E_2 (high) phonon mode and the stress,[16,17] we determine the compressive stresses of -0.91 GPa and -0.56 GPa along the m direction and the c direction from the shifts of E_2 (high) phonon modes 2.47 cm^{-1} and 1.5 cm^{-1} that deviate from the reference frequency in our sample. The negative sign of the stress indicates compression stress. So the stress shows a significant anisotropy and the maximum stress value is along the m axis. Tsuda *et al.*[18] reported that the lattice is contracted along both the c-axis direction and the m-axis direction for nonpolar a-plane GaN, and they also found that the stress in the m-axis direction is larger than that in the c-axis direction. They attributed it to the lattice-mismatch between a-plane GaN and r-plane sapphire, which is only 1% along the c axis and 16% along the m axis.

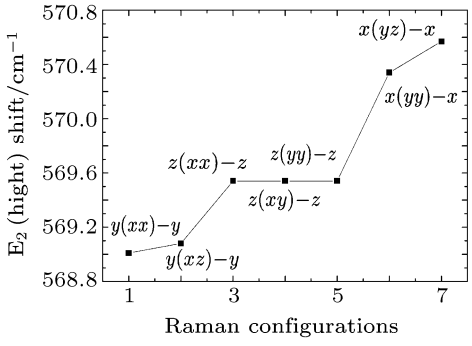


Fig. 4. The frequencies of the E_2 (high) modes of nonpolar a-plane GaN in different scattering configurations.

For the purpose of identifying the effect of difference in stress along different directions on the morphology in our samples, SEM was used to investigate the plane view of the as-grown nonpolar a-plane GaN. On the surface of this sample, a number of cracks were found to appear only along the m axis, as shown in the SEM image in Fig. 5. The slight relaxation of our a-plane GaN occurred only in one direction, which must be due to the much larger stress along the m axis caused during epitaxy. Importantly, it can be clearly seen that there are many triangular pits in the surface of the a-plane GaN, the pits with facets of $(000\bar{1})$ are a typical feature of a-plane GaN, which greatly limits its applications in optoelectronic devices.[19] It seems that the density of the triangular pits relates to the strain relaxation, the number of triangular pits is very small in the surface of the a-plane GaN when a crack appears, the density is very high when no crack occurs. Although the intrinsic source of the triangular pits is unknown at present, the above results seem to show that strain plays an important role.

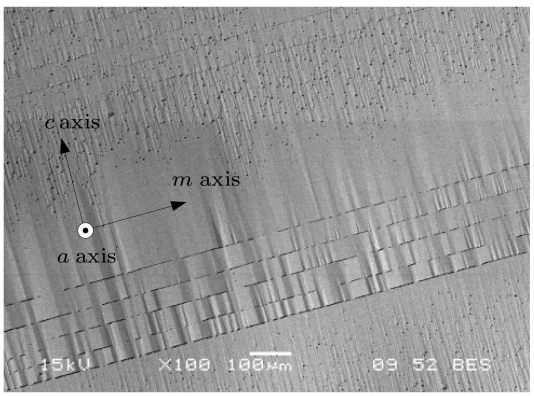


Fig. 5. SEM image of the surface of the nonpolar a-plane GaN layer, showing that the crack is generated is only in the m-axis direction.

Figure 6 shows AFM images of the region near the crack and far away from the crack. The surface of the a-plane GaN after the crack is much smoother than the region without the crack. The surface roughness values in an area of 5 μm×5 μm of the two regions (with and without the crack) are 0.554 nm and 21.1 nm, respectively. One can see that the crack leads to a significant reduction in surface roughness. It is well known that cracks can relieve a significant amount of stress as it often occurs during the growth of the GaN.[8] So, strain has a very important effect on the surface morphology of the a-plane GaN, which is consistent with our previous work in which the AlN/AlGaN strain-management superlattices could improve the morphology of nonpolar a-plane GaN.[6]

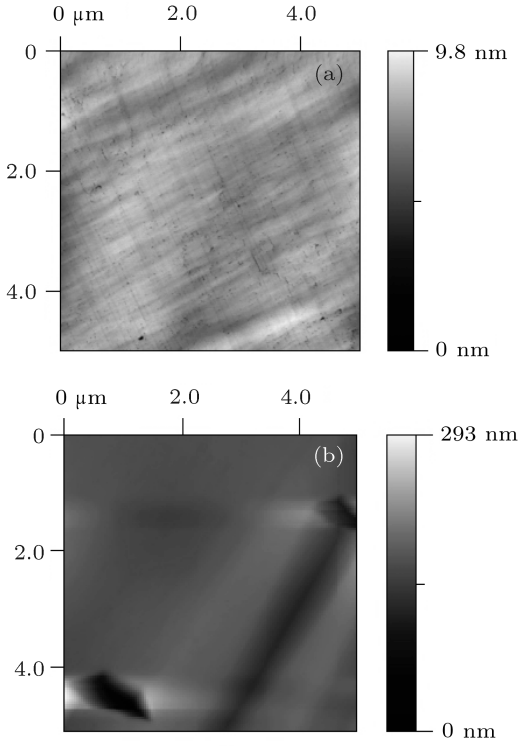


Fig. 6. AFM images of a-plane GaN near the crack region (a) and far away from the crack region (b).

Generally, BSFs relate to the striated surface morphology, the triangle pits, the anisotropic crystalline quality and the presence of an exposed N-face (0002) of GaN as a source of the generation of BSFs.[20] In nonpolar and semipolar GaN, intrinsic (I_1, I_2 and I_3) and extrinsic (E) BSFs can occur in the wurtzite crystal structure. I_1-type BSFs are the most common type of BSF due to their low formation energy, at the same time, I_2- and I_3-type BSFs have higher formation energies and are observed less commonly, I_1-type BSFs are normally bounded by Frank–Shockley PDs ($1/6\langle 20\bar{2}3\rangle$),[21] the reduction of surface roughness and the elimination of triangular pits in the a-plane surface after the relaxation suggest the reduction of the BSFs density. Furthermore, because I_1-type BSFs are normally bounded by Frank–Shockley PDs, the density of PDs must be significant reduced.

4. Conclusions

The Raman scattering spectra of nonpolar a-plane GaN were measured at room temperature in various backscattering geometries from the surfaces and

edges. The frequency values of E_2 (high) modes measured from the $x(\,)$–x, $y(\,)$–y, and $z(\,)$–z are greatly different from each other. This reveals that the strain distribution in nonpolar a-plane GaN is anisotropic. Furthermore, once the direction of the incident light is fixed, the variation of the E_2 (high) mode with polarization direction is not significant. So the anisotropic strain should be calculated according to the direction of incident light. The compressive stresses of -0.91 GPa and -0.56 GPa along the m direction and the c direction in our sample are obtained, therefore, the fact that the cracks occur only along the m axis can be explained. AFM images reveal a significant decrease in both the root-mean-square roughness and the density of submicron pits after the stress relief.

References

[1] Waltereit P, Brandt O, Trampert A, Grahn H T, Menniger J, Ramsteiner M, Reiche M and Ploog K H 2000 *Nature* (London) **406** 865

[2] Xu S R, Hao Y, Zhang J C, Zhou X W, Cao Y R, Ou X X, Mao W, Du D C and Wang H 2010 *Chin. Phys.* B **19** 107204

[3] Zhang J F, Xu S R, Zhang J C and Hao Y 2011 *Chin. Phys.* B **20** 057801

[4] Xu S R, Zhang J C, Li Z M, Zhou X W, Xu Z H, Zhao G C, Zhu Q W, Zhang J F, Mao W and Hao Y 2009 *Acta Phys. Sin.* **58** 5705 (in Chinese)

[5] Imer B, Wu F, Spec J S and DenBaars S P 2007 *J. Cryst. Growth* **306** 330

[6] Xu S R, Hao Y, Zhang J C, Zhou X W, Yang L A, Zhang J F, Duan H T, Li Z M, Wei M, Hu S G, Cao Y R, Zhu Q W, Xu Z H and Gu W P 2009 *J. Cryst. Growth* **311** 3622

[7] Xu S R, Hao Y, Zhang J C, Cao Y R, Zhou X W, Yang L A, Ou X X, Chen K and Mao W 2010 *J. Cryst. Growth* **312** 3521

[8] Roder C, Einfeldt S, Figge S, Paskova T, Hommel D, Paskov P P, Monemar B, Behn U, Haskell B A, Fini P T and Nakamura S 2006 *J. Appl. Phys.* **100** 103511

[9] Lu J Y, Wang Z J, Deng D M, Wang Y, Chen K J, Lau K M and Zhang T Y 2010 *J. Appl. Phys.* **108** 123520

[10] Flissikowski T, Brandt O, Misra P and Grahn H T 2008 *J. Appl. Phys.* **104** 063507

[11] Beechem T, Christensen A, Green D S and Graham S 2009 *J. Appl. Phys.* **106** 114509

[12] Hushur A, Manghnani M H and Narayan J 2009 *J. Appl. Phys.* **106** 054317

[13] Lin H C, Feng Z C, Chen M S, Shen Z X, Ferguson I T and Lu W J 2009 *J. Appl. Phys.* **105** 036102

[14] Wang K R, Ramsteiner M, Mauder C, Wan Q, Hentschel T, Grahn H, Kalisch T H, Heuken M, Jansen R H and Trampert A 2010 *Appl. Phys. Lett.* **96** 231914

[15] Gao H Y, Yan F W, Zhang H X, Li J M, Wang J X and Yan J C 2007 *J. Appl. Phys.* **101** 103533

[16] Song J S, Rho H, Jeong M S, Ju J W and Lee I H 2010 *Phys. Rev.* B **81** 233304

[17] Davydov V Y, Kitaev Y E, Goncharuk I N, Smirnov A N, Graul J, Semchinova O, Uffmann D, Smirnov M B, Mirgorodsky A P and Evarestov R A 1998 *Phys. Rev.* B **58** 12899

[18] Tsuda M, Furukawa H, Honshio A, Iwaya M, Kamiyama S, Amano H and Akasaki I 2006 *Phys. Stat. Sol.* (b) **243** 1525

[19] Ma B, Hu W, Miyake H and Hiramatsu K 2009 *Appl. Phys. Lett.* **95** 121910

[20] Hirai A, Haskell B A, McLaurin M B, Wu F, Schmidt M C, Kim K C, Baker T J, DenBaars S P, Nakamura S and Speck J S 2009 *Appl. Phys. Lett.* **90** 121119

[21] Moram M A, Johnston C F, Hollander J L, Kappers M J and Humphreys C J 2009 *J. Appl. Phys.* **105** 113501